金沢大学
素粒子論研究室

On topological vacuum structure of hot electroweak theory

M.N. Chernodub[1], E.-M. Ilgenfritz[2], A. Schiller[3]

[1]ITEP Moscow, Russia

[2]University of Kanazawa, Japan

[3]University of Leipzig, Germany

3rd Japan-German Seminar Kanazawa, October 15-17, 1999

1. Motivation   Why are the electroweak phase transition (EWPT) and defect mediated mechanisms interesting?
2. Embedded defects in continuum
3. $3D$ lattice model and defect operators
4. Topological vacuum structure at phase transition and crossover
5. Vortex profiles and interactions
6. Summary

Recent work:

- C,Gubarev,I: PLB424
- C,G,I,S: PLB434, PLB443, LATT'98, SEWM'98
- C,I,S: LATT'99, in preparation

Motivation

- Strong interest in 90's in thermodynamic properties of EWPT Standard Model (SM), extended models
- Unimproved perturbation theory fails to describe transition properties depending on the unknown Higgs mass
- Improved perturbation theory and non-perturbative continuum methods can be confirmed by lattice simulations
- Infrared properties of gauge field are essential; by dimensional reduction to $3D$, the crucial soft gauge dynamics is left to be simulated
- Phenomenological background : Viability of baryogenesis (BG) at EWPT?

Assumptions for traditional scenarios of BG

- strong first order phase transition
- transition proceeds by bubble nucleation
- basic BG processes inside bubble walls
- non-erasure by sphalerons after transition requires lower bound for Higgs condensate ($E_{\text{sphal}} \propto |\Phi_{\text{broken}}|$)

$\rightarrow$ How strong is the first order transition?

Main stream lattice calculations
$4D$: Leipzig, DESY–Budapest, Tsukuba
$3D$: Helsinki, Leipzig, Bielefeld

Outcome: Standard model has no true thermal phase transition

$$M_H \text{ lower bound} > M_H^{\text{crit}} = 72 \text{ GeV}$$
$$T^{\text{crit}} = 110 \text{ GeV (with top)}$$

Shift of emphasis

- Alternative models:
  MSSM (Laine, Rummukainen, Budapest)
  External magnetic field (Helsinki-CERN)
- Alternative mechanisms:
  Defect mediated BG (Brandenberger et al., Trodden, Vachaspati)
  As Universe cools down decay of long electroweak strings into smaller, twisted and linked string loops which carry baryon number $B \neq 0$ (first lattice studies by our collaboration)

Three basic defect structures:

- Vortices (on non-contractible sphere in configuration space)
- Nambu monopoles (ends of vortices)
- Sphalerons (saddle point on non-contractible loop in configuration space), a $M\bar{M}$ monopolium state

$\rightarrow$ Vachaspati, Hindmarsh, Klinkhamer, ...

Properties important for observation on lattice:

- Unstable configurations, generated by thermal fluctuations
- can be well studied in thermal equilibrium in region where percolating network of strings is dilute or has already dissolved
- Study of sphaleron properties (constituents) using saddle point cooling

Embedded defects in continuum

- Consider theories with SSB from a Lie group to a subgroup
- vacuum manifold $\mathcal{V}$: space of ground states
- Topological defect: region in space where energy is localized
- In $D = 3$ names monopole, string, domain wall are used for point–like, one–dimensional, two–dimensional defects
- Defects appear for nontrivial homotopy group π_i of $\mathcal{V}$: π_0 – domain wall, π_1 – string, π_2 – monopole

Electroweak model (bosonic sector)

$$\mathcal{L} = \frac{1}{4} G^a_{\mu\nu} G^a_{\mu\nu} + \frac{1}{4} F_{\mu\nu} F^{\mu\nu}$$

$$+ \left| \left(\partial_\mu - \frac{\mathrm{i}}{2} g \sigma^a W^a_\mu - \frac{\mathrm{i}}{2} g' Y_\mu \right) \phi \right|^2 + \lambda \left(\phi^\dagger \phi - \frac{\eta^2}{2} \right)^2$$

Define Z and A fields in terms of arbitrary Higgs configuration $\phi(x)$ suitable for presence of topological defects

$$Z_\mu \equiv \cos\theta_W n^a(x) W^a_\mu - \sin\theta_W Y_\mu$$

$$A_\mu \equiv \sin\theta_W n^a(x) W^a_\mu + \cos\theta_W Y_\mu$$

n^a – isovector order parameter $n^a = -\frac{\phi^\dagger \sigma^a \phi}{\phi^\dagger \phi}$

1. Z–string
   $\pi_1(SU(2)) = 0$, $\pi_1(U(1)) = Z$
   topologically stable classical solution in the $U(1)$ subgroup: Abrikosov–Nielsen–Olesen string from Abelian HM "embedded" into EWM
   carries magnetic flux; Chern-Simons charge contained in a configuration of Z–strings
   Q_{CS} measures twisting of magnetic force lines;
   Z–string terminates on magnetic monopole
2. Nambu monopole
   $\pi_2(SU(2)) = 0$, $\pi_2(SO(3)) = Z$
   topologically stable classical solution of Georgi–Glashow model: "Embedding" of 't Hooft–Polyakov monopole into EWM with n^a field taking rôle of adjoint Higgs field
   no isolated monopoles for monopole–string configuration
3. W–string
   subgroup $U(1)$ entirely lying in $SU(2)$
   $\rightarrow$ W–string can terminate without any emanating electromagnetic field; Z and W–strings coincide up to global gauge transformation for $\theta_W = 0$
4. Sphaleron
   unstable saddle point solution in GSW model with
   $Q_{CS} = B = n_F/2$
   in center of classical sphaleron Higgs field vanishes
   sphaleron: $M\bar{M}$ dipole with a twisted Z–string

   ...

3D lattice model and defect operators

Action

$$S = \beta_G \sum_P \left(1 - \frac{1}{2}\mathrm{Tr}U_P\right) - \beta_H \sum_{x,\mu} \frac{1}{2}\mathrm{Tr}(\Phi_x^\dagger U_{x,\mu}\Phi_{x+\hat{\mu}}) + \sum_x \left(\rho_x^2 + \beta_R(\rho_x^2 - 1)^2\right)$$

with $\rho_x^2 = \frac{1}{2}\mathrm{Tr}(\Phi_x^\dagger \Phi_x)$

Three lattice couplings

- Higgs self coupling $\beta_R \leftrightarrow$ Higgs mass:

$$\beta_R = \frac{\lambda_3}{g_3^2}\frac{\beta_H^2}{\beta_G} = \frac{1}{8}\left(\frac{M_H^*}{80\ \mathrm{GeV}}\right)^2 \frac{\beta_H^2}{\beta_G}$$

- Hopping parameter $\beta_H \leftrightarrow 3D$ mass m_3^2:

$$\beta_H = \frac{2(1-2\beta_R)}{6 + a^2 m_3^2}$$

  with $m_3^2(\mu_3 = g_3^2) = m_3^2 + m_{1-\mathrm{loop}}^2 + m_{2-\mathrm{loop}}^2$ (Laine)
- Gauge coupling $\beta_G \leftrightarrow 3D$ coupling g_3^2:

$$\beta_G = 4/(a g_3^2)$$

g_3^2, λ_3, $m_3(\mu_3)$ *perturbatively known* functions of $4D$ running couplings, M_{Higgs}, T (Kajantie et al.)

Construction of elementary defects

1. take unit isovector (adjoint) composite field
$$n_x = n_x^a \sigma^a \,, \;\; n_x^a = -(\Phi_x^\dagger \sigma^a \Phi_x)/(\Phi_x^\dagger \Phi_x)$$
2. perform Abelian projection
$$V_{x,\mu}(U,n) = U_{x,\mu} + n_x U_{x,\mu} n_{x+\hat{\mu}}$$
   n_x covariantly constant w.r.t. $V_{x,\mu}$
$$n_x V_{x,\mu} = V_{x,\mu} n_{x+\hat{\mu}}$$
3. construct gauge invariant flux through plaquette P
$$\bar{\theta}_P(U,n) = \arg\Big(\mathrm{Tr}\,\big[(\mathbb{1} + n_x) V_{x,\mu} V_{x+\hat{\mu},\nu} V^\dagger_{x+\hat{\nu},\mu} V^\dagger_{x,\nu} \big] \Big)$$
4. obtain a gauge invariant monopole charge j_c inside a cube c as total flux through its surface ∂c
$$j_c = - \sum_{P \in \partial c} \bar{\theta}_P / (2\pi)$$
5. construct Abelian link angles
$$\chi_{x,\mu} = \arg\left(\Phi_x^\dagger V_{x,\mu} \Phi_{x+\hat{\mu}} \right)$$
   and corresponding plaquette angles χ_p
6. define vorticity (similar to Abelian vortices in AHM = Ginzburg–Landau Model)
$$\sigma_P = \left(\chi_P - \bar{\theta}_P \right) / (2\pi)$$

Now, lattice gauge–Higgs field is described as monopole–vortex configuration:

- Vortex formed by links dual to plaquettes carrying non-vanishing vorticity σ_P: ${}^*\sigma_l$
- Vortex trajectories: either closed or begin/end on Nambu (anti-)monopoles:

$$\sum_{\mu=1}^{3} ({}^*\sigma_{x-\hat{\mu},\mu} - {}^*\sigma_{x,\mu}) = {}^*j_x$$

- Vortices form bigger or smaller vortex clusters (networks) depending on the phase

Extended topological defects

- A priori, physical size (or size distribution) of electroweak defects not known:
  for a continuum limit to exist, same size effects should be detected on finer lattices as well
- Use decimated lattice of sites X
  repeat construction for extended V-links:

$$V^{(k)}_{X,\mu} = V_{X,\mu} V_{X+\hat{\mu},\mu} \cdots V_{X+(k-1)\hat{\mu},\mu}$$

  with isovector field n_X covariantly constant, too, when restricted to coarse lattice
- Strategy: compare k–fold finer lattice with $\beta_G \to k\beta_G$ for $(ka)^2$ vortices and $(ka)^3$ monopoles

Topological vacuum structure at phase transition and crossover

- Dual links are *marked* which carry vorticity
- A bond percolation algorithm used to label various disconnected vortex clusters in a given field configuration

1. Observables
   - Densities of monopole ρ_m and vortices ρ_v

$$\rho_m = \sum_c |j_c| / L^3 \qquad \rho_v = \sum_P |\sigma_P| / (3L^3)$$

   - Vortex percolation probability $C = \lim_{r\to\infty} C(r)$

     from a cluster 2–point function (probability to be connected by *one* cluster)

$$C(r) = \frac{\sum\limits_{x,y,i} \delta_{x\in{}^*\sigma(i)} \delta_{y\in{}^*\sigma(i)} \cdot \delta\left(|x-y|-r\right)}{\sum\limits_{x,y} \delta\left(|x-y|-r\right)}$$

   - Cluster length distribution
     length: total number of dual links forming a single connected cluster
   - Cluster multiplicity distribution
     multiplicity: number of distinct connected clusters in a gauge–Higgs configuration

2. At electroweak phase transition

- strongly 1^{st} order: Percolation threshold, densities vanish in Higgs phase, transition at EWPT

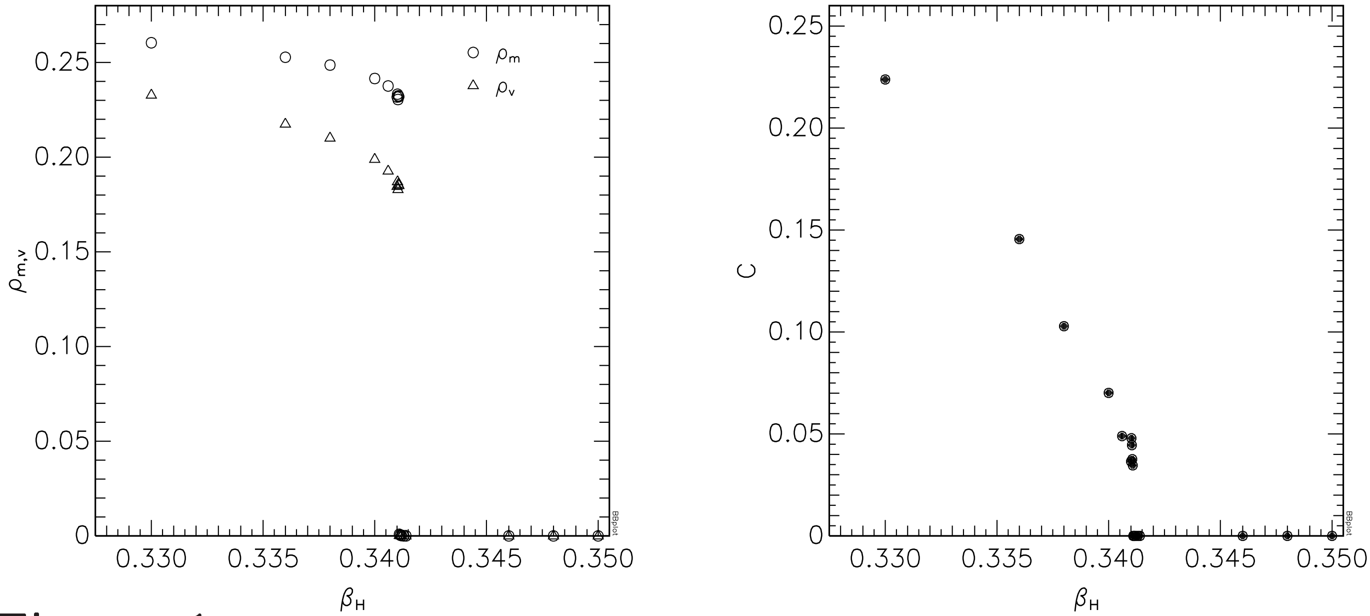

Figure 1: Density of Nambu monopoles ρ_m, of vortices ρ_v and percolation probability C vs. hopping parameter β_H, $M_H^* = 30$ GeV, $\beta_G = 12$.

- weakly 1^{st} order: Percolation threshold, densities extend to Higgs phase

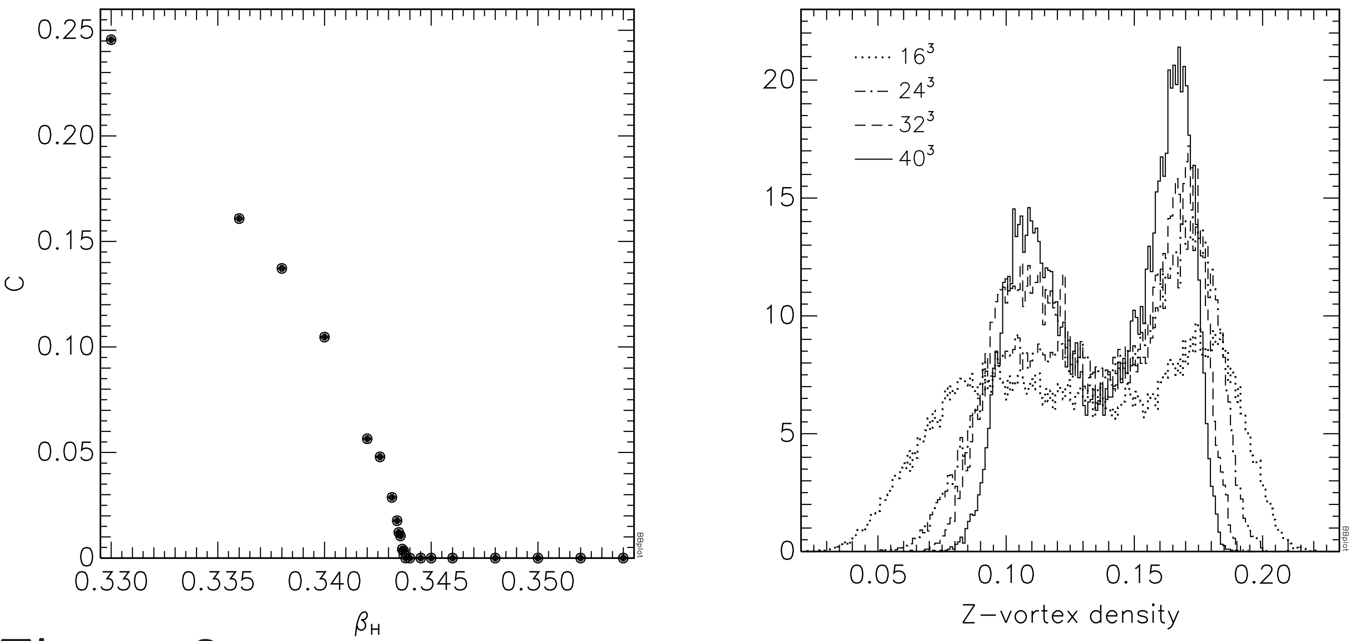

Figure 2: Percolation probability vs. β_H for $M_H^* = 70$ GeV and vortex density distributions at pseudocriticality for different lattice sizes.

3. In the crossover region $M_H^* = 100$ GeV

- Continuum behavior of percolation threshold?
  Percolation threshold at appreciable densities
  At l.c.p. and for fixed physical volume compare defects with extensions $k = 1 \to 2 \to 3$ for sizes $16^3 \to 32^3 \to 48^3$ and $\beta_G = 8 \to 16 \to 24$,
  $\to$ threshold corresponds to same T
  $T^{\text{perc}} \approx 130$ GeV, $M_H \approx 103$ GeV (with top)
  Percolation transition at crossover parameters
- Change of vortex cluster structure similar for all vortex thicknesses $(ka)^2$
  $\to$ average length per cluster drops to a plateau, then changes slowly with T
  $\to$ multiplicity of distinct clusters maximal at crossover temperature

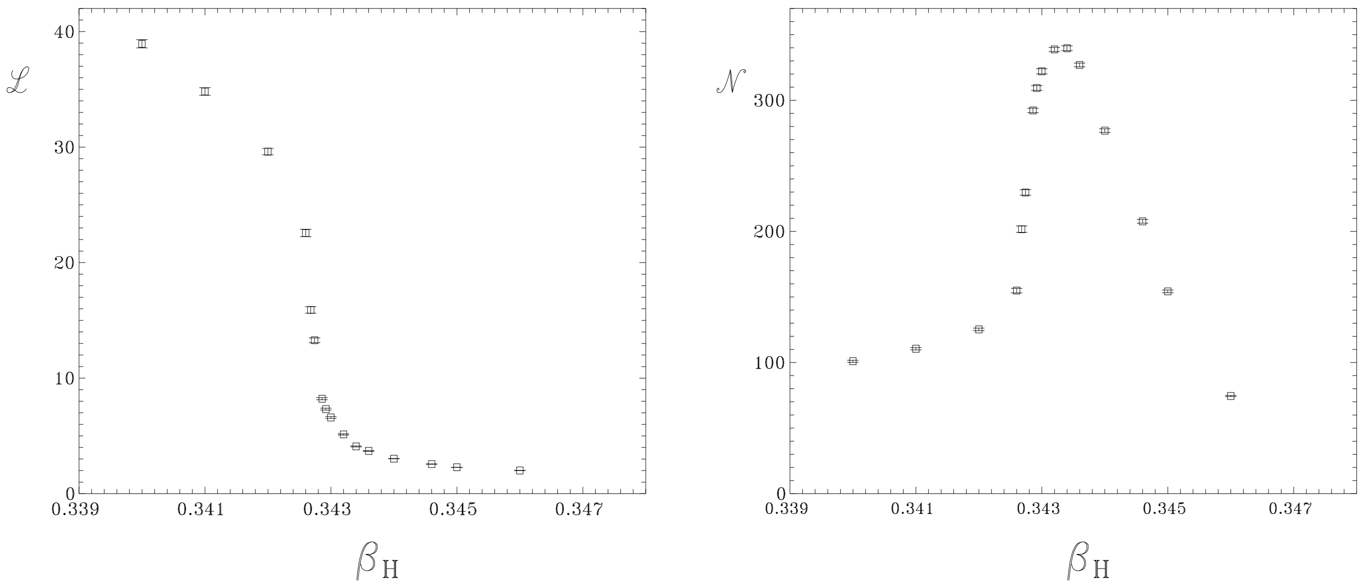

Figure 3: Average length $\mathcal{L}$ per vortex cluster and average number $\mathcal{N}$ of vortex clusters per configuration (size $k = 2$, 32^3, $\beta_G = 16$)

- Suggested scenario: percolating clusters decay into smaller ones (vortex rings and monopolium) $\rightarrow$ kinetic approach to crossover
  at still smaller T rings disappear but pairs still survive
  tail: interpret $\rho_v/2$ partly (twist ?) as sphaleron density on broken side
  conjecture supported by signatures of classical sphaleron

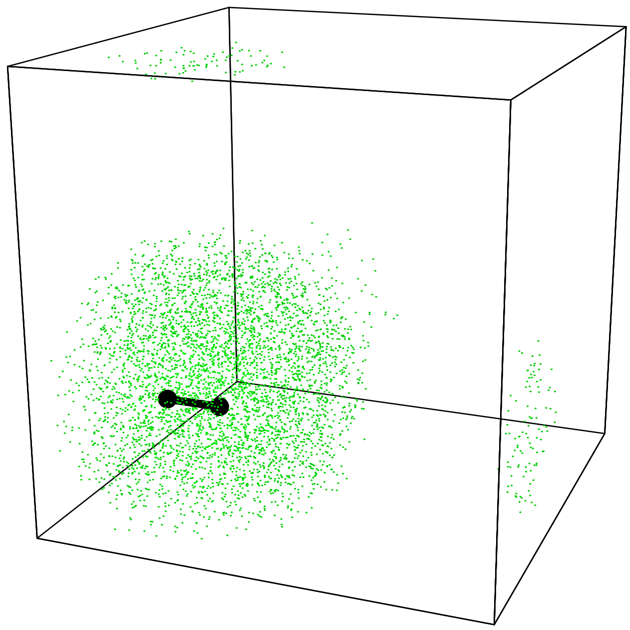

Figure 4: Classical sphaleron as a Nambu monopolium bound by a vortex string. The clouds show the suppression in Higgs field modulus.

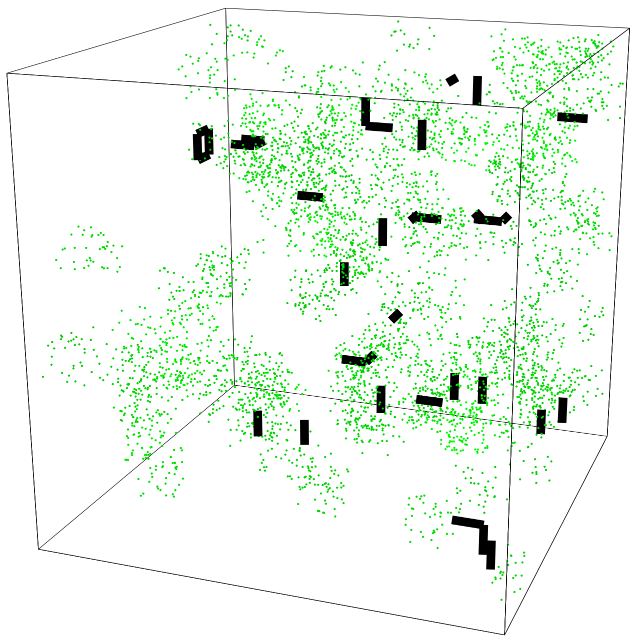

Figure 5: Clusters of extended (k = 3) vortices just below T_{perc}. The Higgs modulus is visualized as before. The snapshot shows large quantum fluctuations around defect position.

Vortex profiles and interactions

continuum: at center of vortex zero Higgs field modulus, maximal energy density
$\rightarrow$ if vacuum populated by vortex-like configurations find lines of Higgs field zeroes and maximal energy density

Topologically unstable vortices populate the "vacuum" due to thermal fluctuations
not expected to find vortices with classical (ANO type) profiles
vortex profile around vortex line position screened by quantum fluctuations
average over all vacuum vortices may reveal structure resembling classical vortex to some extent
$\rightarrow$ study correlators of vortex operators with gauge invariant field operators – quantum vortex profiles

Questions of interest:

- Is there a relevant volume fraction staying in the wrong (symmetric) phase (sustaining rapid B violating processes) after the transition?
- How does the profile and the interaction of vortices change with T?

Vortex profiles

clearly seen different behavior near to vortex trajectory and outside, larger effect on Higgs side (vortices dilute)

Correlator study for a more detailed insight

Vortex–field correlators

$$C_\rho(R) = \langle \sigma^2_{P_0}\, \rho^2_{P_R} \rangle\,, \qquad C_E(R) = \langle \sigma^2_{P_0}\, E^g_{P_R} \rangle$$

R distance between plaquettes, $\rho^2_P = (1/4)\,\sum_{x\in P} \rho^2_x$

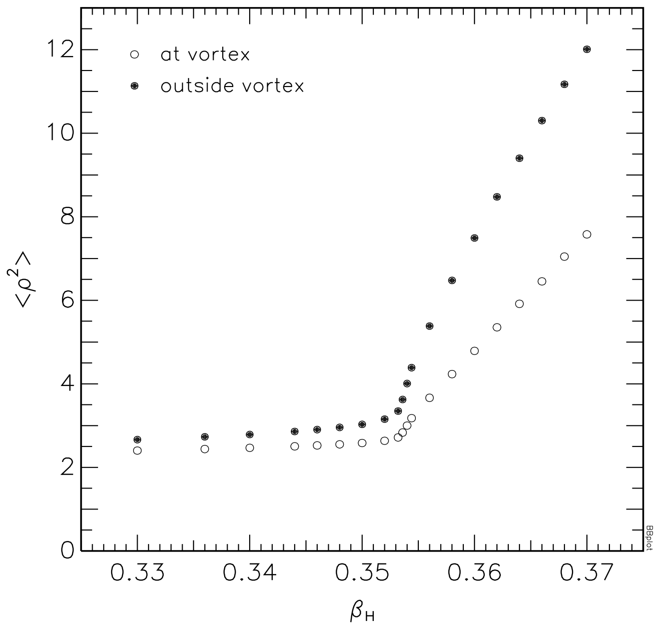

Figure 6: The squared Higgs modulus inside and outside of a vortex *vs.* β_H, $M_H^* = 100$ GeV, 16^3, $\beta_G = 8$.

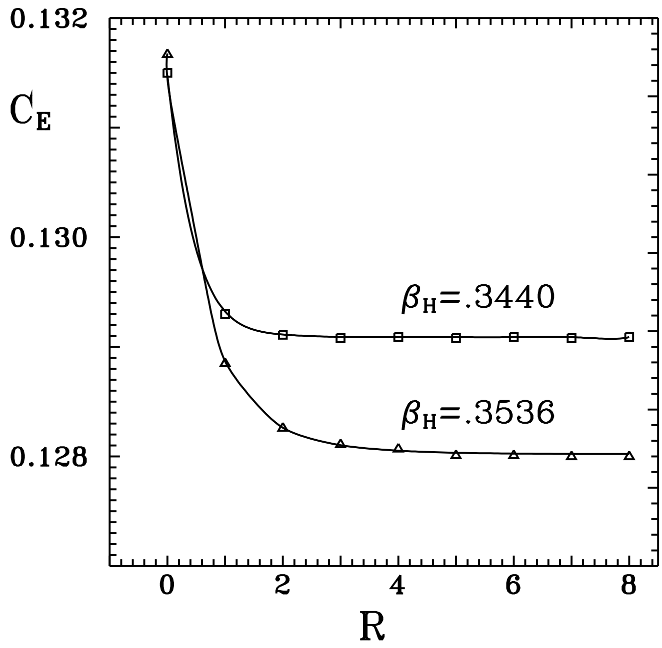

Figure 7: Examples of quantum vortex profiles for the gauge field energy. Solid lines represent fits.

Effective "photon" mass near crossover

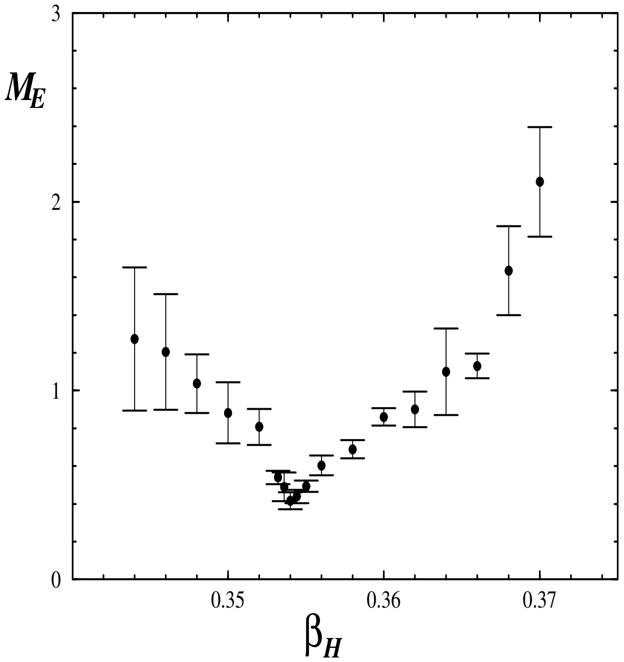

Figure 8: Lattice "photon" mass from vortex energy profile vs. β_H, $\beta_G = 8$.

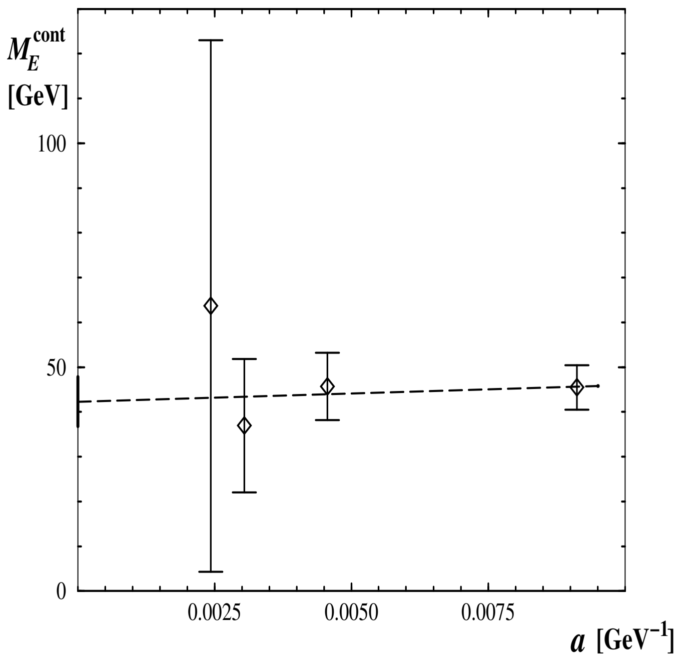

Figure 9: Continuum limit for "photon" mass on top of the crossover.

Localization of Higgs zeroes from extended vortex construction?

Type of vortex vacuum

Vortex-vortex correlators

$$\langle|\sigma_{P_0}|\,|\sigma_{P_R}|\rangle = 2\,(g_{++} + g_{+-})$$
$$\langle\sigma_{P_0}\,\sigma_{P_R}\rangle = 2\,(g_{++} - g_{+-})$$

$g_{+\pm}$: contributions to of parallel/anti–parallel vortices at positions P_0 and P_R

$g_{++}(R)$: average density of vortices (anti-vortices) relative to bulk density in plane orthogonal to vortex current at distance R; long range tail should exponentially approach unity from above/below if vortices attract/repel each other (type–I/type–II)

$g_{+-}(R)$: attractive, independent of superconductivity type

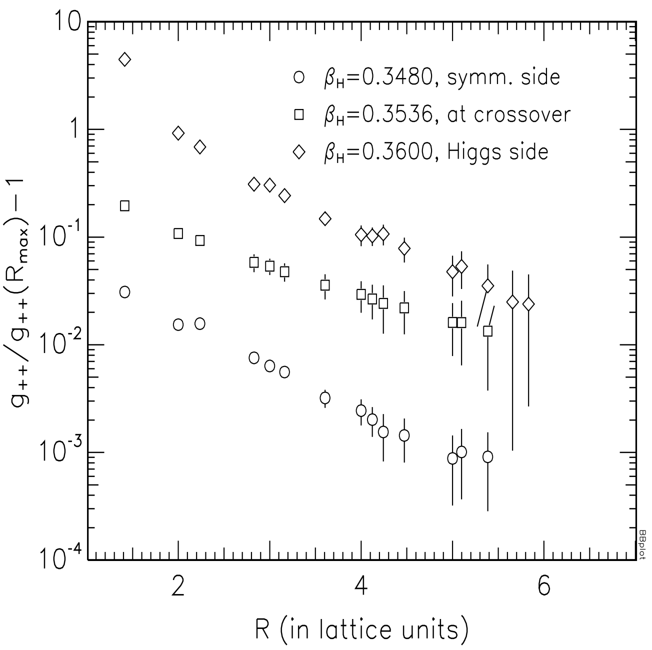

Figure 10: Normalized correlator $g_{++}(R)$, 16^3, $\beta_G = 8$.

Result: Electroweak matter near crossover belongs to type–I vortex vacuum class, attractive character stronger on Higgs side

Summary

- First order EWPT accompanied by percolation transition of topological *embedded* defects which are observed for the first time in lattice simulations
- Percolation transition persists in EW crossover region (for realistic Higgs masses)
- Percolating networks of vortex string omnipresent for $T > T_{\rm perc}$, at $T < T_{\rm perc}$ vortices form dilute gas of closed vortex loops and Nambu $M\bar{M}$ states, further below $T^{\rm perc}$, small vortex loops shrink and disappear while $M\bar{M}$ pairs still survive
- Some part of these pairs can be associated with sphaleron–like configurations known to exist in the broken phase
- Quantum vortices have a physical "thickness" ("photon" mass)
- The vortex dynamics is governed by a type-I effective Ginzburg–Landau superconductive model
- Although ruled out as an alternative of BG within the Standard Model, defect mechanisms remain interesting within extended models (if the phase transition is too weak)
- Study of topological defects in lattice models developed for EWPT is an interesting new topic, overlapping interest with cosmologists and solid state physicists